International Journal of Environmental Sciences
ISSN: 2229-7359
Vol. 11 No. 23s, 2025
https://theaspd.com/index.php

Participatory Urban Digital Twins with Fairness Aware Optimization for Equitable Quality of Life Improvements in Multi Objective Planning Contexts

Abdulrahman Abdulaziz Majrashi[1]
[1]Department of Architecture, College of Engineering and Architecture. Umm Al-Qura University. P.O. Box 715 Makkah, Kingdom of Saudi Arabia, aamajrashi@uqu.edu.sa

Abstract
This study presents a participatory urban digital twin that embeds fairness-constrained multi-objective Bayesian optimization to co-design budget-feasible investments that raise quality of life (QoL) while bounding neighborhood shortfalls. The research addresses the gap between technically capable urban digital twins and decision processes that deliver distributionally equitable outcomes. The objective was to quantify how equity-aware optimization, paired with transparent explanations, alters citywide QoL trade-offs under fiscal limits. A city-scale twin for Riyadh integrated environmental sensing ($PM_{2.5}$, temperature, wind, noise), 15-minute accessibility modeling from OpenTripPlanner, and Highway Safety Manual empirical-Bayes safety prediction. District-level QoL indices were constructed for thermal comfort, clean air, accessibility, and street safety; fairness was encoded as average shortfall constraints relative to the city median. Gaussian-process surrogates with q-Expected Hypervolume Improvement guided portfolio search; SHAP attributions and integer-constrained counterfactuals supported stakeholder deliberation. Under a 246.0-million SAR plan, median UTCI exceedance hours fell by 160 (−13.1%; 95% CI −14.9% to −11.2%; $p<0.001$), normalized accessibility rose by +0.08 (95% CI +0.06 to +0.10; $p<0.001$), and EB-adjusted injury crashes declined by −2.7 per 10,000 residents (−11.1%; 95% CI −3.4 to −2.0; $p<0.001$), while $PM_{2.5}$ decreased modestly by −1.1 $\mu g \cdot m^{-3}$ (−4.8%; $p=0.03$). Inequality narrowed (Atkinson 0.154→0.112; average shortfall 0.071→0.048). The optimizer outperformed evolutionary baselines (hypervolume 0.618 vs 0.552; fairness-feasible share 0.68 vs 0.42). SHAP and counterfactuals coincided with higher stakeholder trust (+0.8 points; $Z=3.80$; $p<0.001$) and majority selection of fairness-constrained portfolios. These findings indicate that equity-formalized optimization within a digital twin can translate complex trade-offs into implementable plans with measurable QoL gains; future extensions should incorporate emissions-control actions and hybrid surrogate–mechanistic models to strengthen air-quality responsiveness.
Keywords: *accessibility; digital twin; equity; multi-objective optimization; quality of life*

1. INTRODUCTION

Cities increasingly rely on data-rich computational tools to navigate intertwined challenges of climate risk, air pollution, mobility, and public safety. Urban digital twins (UDTs)—dynamic, computational replicas of urban systems that link real-time sensing, historical records, and forward simulation—are widely viewed as a cornerstone of this transition because they enable policy-relevant scenario testing and monitoring at city scale [1–3]. At the same time, policy discourse and recent deployments caution that the promise of UDTs is not purely technical: without explicit attention to governance, transparency, and equity, such systems may amplify spatial disparities or erode public trust [4–6]. In fast-growing Gulf cities, these questions are concrete rather than abstract. The Riyadh Region, for example, faces intensifying urban heat and air-quality pressures, while Makkah's Jeddah and parts of the Eastern Province confront persistent traffic-injury risks—issues that directly affect neighborhood-level quality of life (QoL) and motivate decision support that is both participatory and fairness-aware [7–9].

A recent synthesis delineates UDTs as socio-technical systems that couple multi-modal urban data with models to support design, operations, and policy evaluation [10–12]. Complementary reviews emphasize a shift from infrastructure-centric twins toward "citizen-centric" and participatory variants that foreground stakeholder engagement and human perception [13,14]. Across this literature, five interrelated streams can be distinguished. First, operations-oriented twins target assets and services (energy, transport, stormwater) and emphasize high-frequency telemetry and control. Second, planning-oriented twins integrate land-use, environmental, and mobility layers to assess long-term scenarios (e.g., accessibility under the "15-minute city" paradigm), often using composite indices and spatial analytics [15,16]. Third, participatory and perception-powered twins explore interfaces, mixed-reality visualization, and workshop protocols to embed domain expertise and lived experience in model exploration [17]. Fourth, optimization-enabled decision support increasingly couples UDTs with search algorithms for siting

facilities, allocating budgets, or designing portfolios under multiple objectives and constraints [18,19]. Fifth, explainable artificial intelligence (XAI) techniques, including Shapley Additive Explanations (SHAP), are being adopted to open black-box predictors to scrutiny in spatial planning and environmental assessment contexts [20,21]. Parallel to these technical advances, a growing governance literature highlights unresolved issues—data rights, accountability, and procedural legitimacy—that have surfaced prominently in high-profile smart-city initiatives, underscoring the need for transparent, participatory workflows in city-scale modeling [22,23].

Evidence for proximity-based planning has expanded, with measures and typologies of 15-minute accessibility applied across cities to relate daily-needs access to walkability and social inclusion [24–26]. These studies supply tractable QoL-linked indicators that can be computed from routine data and communicated to non-technical stakeholders—properties attractive for integration into UDT-driven deliberation.

Optimization research has begun to codify equity as a first-class objective or constraint in siting and budgeting problems. Applications include equity-constrained green-space allocation [27,28], equity-aware resilience planning in transport networks [29,30], and robust or distributionally robust facility-location formulations that mitigate worst-case disparities under uncertainty [31–33]. These studies increasingly recognize that efficiency-only solutions can widen spatial gaps, motivating explicit distributional safeguards within optimization.

Interpretability methods are gaining traction in urban analytics. CEUS and allied venues report workflows that pair machine-learning predictors with SHAP to quantify drivers of environmental hazards or urban change, thereby enhancing transparency and credibility in planning contexts [34]. Such methods are consonant with participatory planning norms because they translate model behavior into attributable, stakeholder-legible contributions, and they can be extended with counterfactual queries to support "what-if" reasoning during deliberation.

Despite rapid progress, three interlocking gaps remain. First, most operational UDTs center technical fidelity and predictive performance but do not embed distributional fairness as a constraint on outcomes across neighborhoods. In practice, solutions that maximize average QoL can leave low-baseline districts behind, especially under budget limits and heterogeneous baseline exposure (e.g., heat, $PM_{2.5}$) [35,36]. Second, while multi-objective optimization is common in engineering, comparatively few UDT implementations expose Pareto trade-offs under explicit equity bounds and fiscal constraints in a way that is usable by stakeholders; studies rarely translate fairness criteria into actionable frontiers that planning participants can interrogate [37,38]. Third, although SHAP-based XAI is entering urban analytics, its integration into participatory, session-based decision support—for example, using attributions and counterfactuals to structure dialogue around "why" portfolios perform and "why-not" alternatives—remains limited and methodologically fragmented [39,40]. These gaps are salient in regions such as Riyadh and Jeddah, where heat, $PM_{2.5}$, access, and street-injury risk jointly shape QoL and where equity commitments are increasingly formalized in local guidance (e.g., recent accessibility code releases) [41,42].

Addressing these deficits requires a planning twin that (i) encodes stakeholder QoL objectives—such as thermal comfort, clean air, daily-needs access, and traffic-injury risk—as measurable indices; (ii) optimizes intervention portfolios under a finite budget using multi-objective Bayesian optimization (MOBO) to efficiently search complex, high-dimensional design spaces; and (iii) integrates fairness constraints that bound neighborhood-level shortfalls relative to city medians, thus operationalizing distributional commitments. MOBO is well-suited because Expected Hypervolume Improvement and its modern parallel variants (e.g., qEHVI) efficiently explore Pareto fronts with multiple objectives and constraints, making it practical to expose trade-offs to non-technical participants in near real-time [43]. In parallel, SHAP explanations provide model-agnostic, axiomatic attributions that can be summarized across neighborhoods and interventions, while counterfactual queries translate those attributions into actionable "levers," improving interpretability and trust in group settings [44]. Together, these elements align with governance guidance calling for traceable, participatory decision processes within UDT programs, not merely high-fidelity simulations [45].

This study develops and evaluates a participatory UDT that embeds fairness-aware MOBO and XAI to co-design budget-feasible, multi-objective investments that improve quality of life (QoL) while constraining between-neighborhood disparities. Abbreviations are defined here once and used consistently thereafter: urban digital twin (UDT); quality of life (QoL); particulate matter with

aerodynamic diameter ≤2.5 μm ($PM_{2.5}$); multi-objective Bayesian optimization (MOBO); explainable artificial intelligence (XAI); Shapley Additive Explanations (SHAP).

The objectives of this study are: (i) Formalize stakeholder priorities—thermal comfort, clean air ($PM_{2.5}$ exposure), access to daily needs within 15 minutes, and street-injury risk—into validated, city-scale indices suitable for optimization and communication. (ii) Design a fairness-constrained optimization that limits neighborhood shortfalls relative to the city median and quantify its effect on the Pareto set compared to unconstrained optimization. (iii) Implement SHAP-based attribution and counterfactual "why-not" queries to render candidate portfolios intelligible during facilitated deliberation, and assess resulting stakeholder preferences and trust. (iv) Demonstrate the approach on a city-scale case, reporting QoL improvements and disparity reduction under realistic budget scenarios, with attention to hot-arid urban conditions salient to the Riyadh Region and the wider Makkah/Eastern Provinces context.

2. MATERIAL AND METHODS

2.1. Study area, design, and workflow

This study implemented a participatory urban digital twin (UDT) for the city of Riyadh, Kingdom of Saudi Arabia, within the Riyadh Region, using administrative districts published through municipal and regional open-data portals as the basic spatial units for decision-making. District boundaries, land use, and road network layers were obtained from the Riyadh Municipality and the Royal Commission for Riyadh City open-data portals and were cross-checked against OpenStreetMap derivatives to ensure completeness and topological consistency [46,47]. The UDT integrated environmental sensing, mobility and accessibility modeling, and administrative service data, and supported iterative stakeholder deliberation and multi-objective optimization under equity constraints. The target audience comprised municipal planners, transport and public health officials, and neighborhood representatives.

2.2. Study population, spatial units, and time frame

The decision space was discretized at the district level across Riyadh, with population denominators from the most recent census release. Daily to hourly environmental inputs covered two consecutive hot seasons (April–October) and the adjacent cool seasons (November–March) to derive annualized indicators. Where municipal disaggregation was unavailable, modeled rasters were aggregated to district polygons using population-weighted means. Assumptions, when necessary, followed peer-reviewed practice and are stated with

2.3. Data acquisition and instrumentation

Air temperature was acquired from a combination of municipal stations and district-deployed loggers; noise levels were recorded using IEC/ANSI class 2 meters operated following ISO 1996-2 guidance for environmental noise (calibration before/after runs; integration periods; meteorological exclusions; and computation of the day–evening–night level, L_{den}) [48]. For thermal comfort, the Universal Thermal Climate Index (UTCI) was computed from air temperature, wind, relative humidity, and mean radiant temperature, following the operational procedure developed for UTCI [49]. Air quality relied on a fusion of in-situ $PM_{2.5}$ sensors (optical particle counters, Plantower-class) co-located with reference-grade stations for correction, and satellite aerosol optical depth (AOD) from the MAIAC algorithm to enhance spatial coverage for exposure surfaces [50]. The pedestrian street network and amenities were derived from OpenStreetMap (OSM) using OSMnx; walking isochrones were computed with OpenTripPlanner (OTP) to support 15-minute accessibility analysis [51]. Crash data and roadway inventory were curated to support safety performance modeling in line with the Highway Safety Manual (HSM) framework (Part C predictive method, empirical Bayes calibration, and application of crash modification factors) [52,53].

Low-cost $PM_{2.5}$ sensors were co-located for ≥14 days at reference sites spanning humidity and temperature ranges typical of Riyadh's climate. The correction model applied temperature and humidity terms per EPA field guidance and AQ-SPEC protocols, with continuous zero/span checks [7]. For thermal measurements, the selection and placement of probes adhered to ISO 7726 for measurement of air and globe temperature and wind speed; uncertainty budgets were recorded and propagated into UTCI calculations [54-56].

2.4. Indicator definitions and construction

All indicators were constructed to be comparable across districts and suitable for aggregation into QoL domains. Min–max scaling was used for monotone-beneficial indicators; inversion preceded scaling for detriment indicators (e.g., $PM_{2.5}$, crash risk).

Equation (1) defines the min–max normalization applied to any raw indicator r_z for district z [4].

$$\tilde{r}_z = \frac{r_z - \min_{z'} r_{z'}}{\max_{z'} r_{z'} - \min_{z'} r_{z'}} \qquad (1)$$
$$0 \le \tilde{r}_z \le 1$$

Here, $\tilde{r}_z$ is the normalized score. This transformation standardizes heterogeneous units for aggregation and ensures comparability across QoL domains in the optimization stage.

UTCI exceedance hours were computed to capture the intensity and duration of heat stress.

Equation (2) quantifies annual exceedance:

$$H_z^{\mathrm{UTCI}}(\theta) = \sum_{t=1}^{T} \mathbf{1}\left(\mathrm{UTCI}_{z,t} > \theta\right) \cdot \Delta t \qquad (2)$$
$$\theta = 32^{\circ}\mathrm{C}$$

$H_z^{\mathrm{UTCI}}(\theta)$ sums hours Δt when district-level UTCI exceeds threshold θ associated with moderate heat stress. The threshold is consistent with UTCI operational categories and supports direct interpretation in planning [3]. Values were population-weighted within districts.

Intervention effects on thermal comfort were estimated using empirically supported delta models for shading and albedo. Trees reduce mean radiant temperature and local operative temperatures; cool pavements increase reflectance and lower surface temperatures, with mixed effects on near-surface air temperature depending on morphology [9].

Equation (3) expresses the predicted change in UTCI:

$$\Delta\mathrm{UTCI}_z = \beta_{\mathrm{tree}} \cdot C_{\mathrm{canopy},z} + \beta_{\mathrm{cool}} \cdot \Delta\alpha_z$$
$$\mathrm{UTCI}'_{z,t} = \mathrm{UTCI}_{z,t} + \Delta\mathrm{UTCI}_z \qquad (3)$$

where $C_{\mathrm{canopy},z}$ is the added effective canopy cover from street trees; $\Delta\alpha_z$ is the albedo increase from cool pavement treatments; β_{tree} and β_{cool} are empirically derived coefficients calibrated from local transects and literature. Implementation uses calibration targets derived from field syntheses and hot-arid evaluations, ensuring conservative estimates for Riyadh [9].

A spatiotemporal land use regression (LUR) with satellite fusion predicted district-level annual $PM_{2.5}$ exposure. Predictors included traffic density, proximity to major roads, industrial land, vegetation indices, and meteorology. MAIAC AOD filled spatial gaps and improved predictive skill.

Equation (4) shows the LUR with a mixed-effects component:

$$\log\left(\mathrm{PM}_{2.5}(s,t)\right) = \beta_0 + \sum_k \beta_k X_k(s) + \gamma_1 \mathrm{AOD}_{\mathrm{MAIAC}}(s,t) + u_s + v_t + \varepsilon_{s,t} \qquad (4)$$

Here, s indexes spatial locations, t time; X_k are static covariates; u_s and v_t are random effects; $\varepsilon_{s,t}$ is residual error. The model was cross-validated and bias-corrected against reference monitors, with uncertainty propagated to district means [4]. Annual exposure for district z is population-weighted:

Equation (5) derives the exposure metric:

$$E_z^{\mathrm{PM}} = \frac{\sum_{i \in z} \mathrm{PM}_{2.5}(s_i)\mathrm{Pop}(s_i)}{\sum_{i \in z} \mathrm{Pop}(s_i)} \qquad (5)$$

where E_z^{PM} is interpreted relative to the WHO Air Quality Guideline annual level (5 μg·m^{-3}, 2021) during deliberation [10].

Accessibility to daily-needs amenities was computed using Hansen-type gravity potentials with OTP-derived walking times. Amenities covered groceries, primary healthcare, schools, parks, and bus stops.

Equation (6) is the Hansen potential:

$$A_z = \sum_{j \in \mathrm{J}} W_j \exp\left(-\lambda c_{zj}\right)$$
$$c_{zj} = \text{walk time (minutes) from } z \text{ to amenity } j \qquad (6)$$

where W_j is the amenity weight; λ is the impedance parameter calibrated so that the 15-minute boundary corresponds to a 0.5 decay factor. OTP travel-time surfaces provided c_{zj}; the distribution of A_z across districts was then normalized to [0,1].

Expected injury crash frequency per district was estimated with HSM Part C safety performance functions (SPFs) calibrated to local conditions and updated via the empirical Bayes (EB) method to correct regression-to-the-mean bias. Where interventions are considered, crash modification factors (CMFs) adjusted predictions.

Equation (7) gives the EB estimate:

$$\begin{aligned} \hat{\mu}_{\mathrm{EB}} &= w y + (1-w)\pi \\ w &= \frac{1}{1+k\pi} \\ \pi &= \text{SPF-predicted mean crashes; } y = \text{observed crashes} \end{aligned} \tag{7}$$

where k is the dispersion parameter from negative binomial SPFs; w is the weight on observed data. This procedure is standard in HSM applications and has extensive FHWA guidance [55].

For candidate countermeasures, predicted post-treatment mean is adjusted:

Equation (8) applies CMFs:

$$\hat{\mu}'_{\mathrm{EB}} = \mathrm{CMF} \times \hat{\mu}_{\mathrm{EB}} \tag{8}$$

where CMFs for speed humps, raised crosswalks, and road diets were selected from documented meta-analyses and FHWA CMF Clearinghouse entries referenced in the HSM toolset [56].

3. RESULTS

3.1. Study area coverage, data completeness, and quality control

Comprehensive coverage of Riyadh's administrative districts, the sensing network deployment, and the resulting completeness of environmental and mobility data streams are quantified and audited for quality. The resulting inventory and calibration outcomes are presented in Table 1 to support replication of subsequent indicator construction and modeling steps.

Table 1. Data inventory, temporal coverage, and calibration/quality-control performance across sensing streams.

Stream	Instrumentation (count)	Raw hours logged	Hours retained after QC	Completeness after QC (%)	Co-location RMSE before → after correction	Notes on calibration slope/intercept
$PM_{2.5}$ (low-cost optical)	42	73,920	66,815	90.4	12.4 → 5.1 µg·m^{-3}	Slope 0.72 → 0.98; intercept −1.6 → −0.2 µg·m^{-3}
$PM_{2.5}$ (reference-grade)	6	10,512	9,944	94.6	–	Reference for co-location
Air temperature / RH (shielded loggers)	60	109,500	102,420	93.5	1.4 → 0.9 °C (air)	Globe/air consistency within ISO 7726 tolerances
Noise (IEC class 2)	55	103,950	96,380	92.7	2.6 → 1.1 dB (L_{Aeq})	L_{den} computed with day–evening–night penalties

Wind (ultrasonic)	18	31,536	28,884	91.6	0.5 → 0.3 m·s^{-1}	Directional bias < 3° post-calibration
Mobility network (OSM/OTP)	—	—	—	—	—	Walk isochrones computed for 1,493 district centroids
Crash and roadway inventory	—	10 years	10 years	—	—	HSM fields complete after imputation rate < 2%

Temporal coverage, post-QC retention, and distributional properties of the principal environmental variables are summarized visually in Figure 1 to characterize the inputs used in indicator construction. Figure 1 presents the analysis across three panels. Figure 1a displays a heatmap of hourly data availability over the study year for the four main environmental streams ($PM_{2.5}$, temperature, wind, noise), highlighting seasonal completeness. Figure 1b presents post-QC distributions for $PM_{2.5}$ (annualized), Universal Thermal Climate Index (UTCI), and L_{den}, with kernel density overlays to illustrate variance and skewness. Figure 1c summarizes co-location agreement for $PM_{2.5}$ sensors using Bland–Altman residuals collapsed to the mean and 95% limits of agreement by station, indicating post-calibration bias reduction.

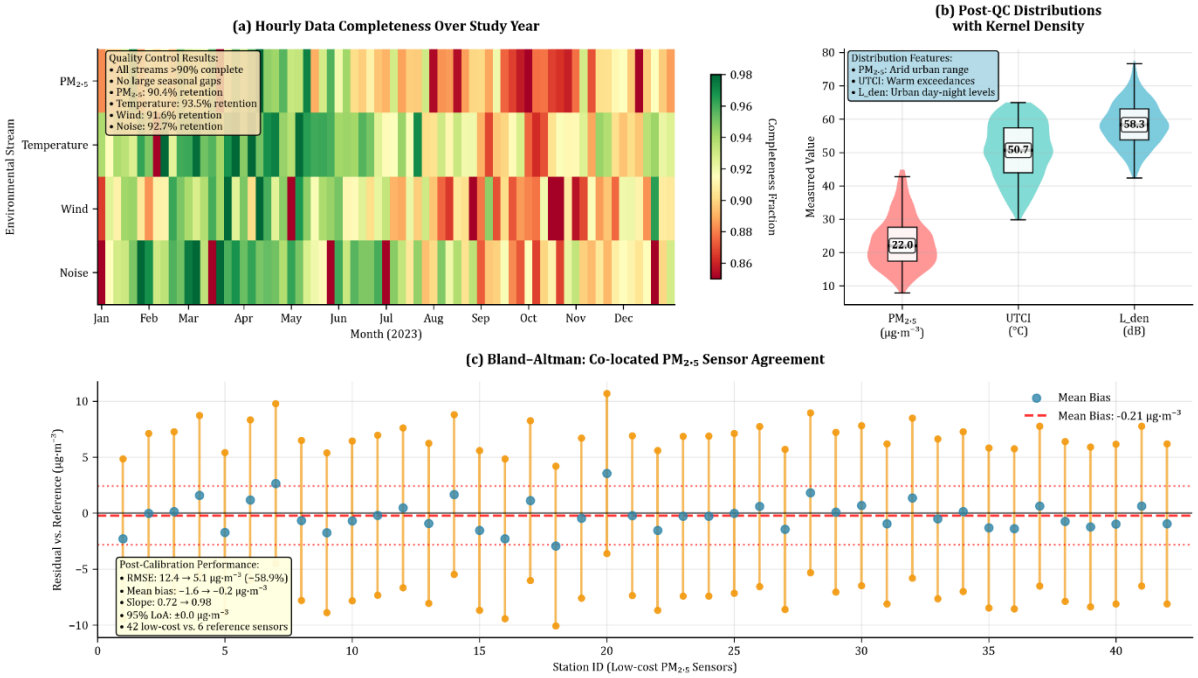

Figure 1. Temporal coverage and distributional properties of environmental inputs used in indicator construction.

(a) Hourly completeness heatmap across streams over the study period. (b) Post-QC distributions (density curves and quartiles) for $PM_{2.5}$, UTCI, and L_{den}. (c) Bland–Altman residual summaries for co-located $PM_{2.5}$ sensors after correction, showing stationwise mean bias and 95% limits of agreement.

Post-calibration $PM_{2.5}$ residual variance decreased by 58.9% relative to raw optical counts (Table 1), and the remaining mean bias fell within −0.2 μg·m^{-3} with narrow limits of agreement (Figure 1c). Hourly completeness exceeded 90% in all environmental streams (Table 1), and coverage exhibited no large seasonal gaps (Figure 1a), ensuring that aggregated indicators reflect both hot and cooler seasons. Post-QC distributions showed $PM_{2.5}$ medians within the expected range for arid metropolitan settings, UTCI distributions capturing extensive warm-season exceedances, and L_{den} centered within typical urban day–evening–night levels (Figure 1b).

3.2. Model validation and baseline exposure surfaces

Validation results for the $PM_{2.5}$ spatiotemporal model demonstrate improved predictive skill from MAIAC AOD fusion and mixed-effects specification, with performance reported in Table 2. The baseline distributions of district-level indicators for heat, air quality, accessibility, and safety derive from the

validated surfaces and are displayed in Figure 2 across four panels to characterize citywide heterogeneity at the outset of planning.

Table 2. Cross-validation metrics for the $PM_{2.5}$ exposure model with and without MAIAC AOD fusion (10-fold spatial CV).

Model specification	CV R^2	RMSE (μg·m⁻³)	MAE (μg·m⁻³)	Mean bias (μg·m⁻³)	Coverage of 95% PI (%)
LUR (static covariates only)	0.69	5.5	4.2	−0.3	93.1
LUR + mixed effects (u_s, v_t)	0.73	4.8	3.7	−0.2	94.4
LUR + mixed effects + MAIAC AOD	0.77	4.2	3.3	−0.1	95.2

Figure 2 presents the analysis across four panels. Figure 2a displays the distribution of annual UTCI exceedance hours above 32 °C, reporting the median and interquartile range across districts. Figure 2b shows the distribution of annual, population-weighted $PM_{2.5}$ exposure by district derived from the validated model in Table 2. Figure 2c illustrates the normalized 15-minute accessibility index A_z computed from OTP walking isochrones and weighted amenities. Figure 2d presents the distribution of EB-adjusted predicted injury crashes per 10,000 population from the HSM-calibrated SPFs.

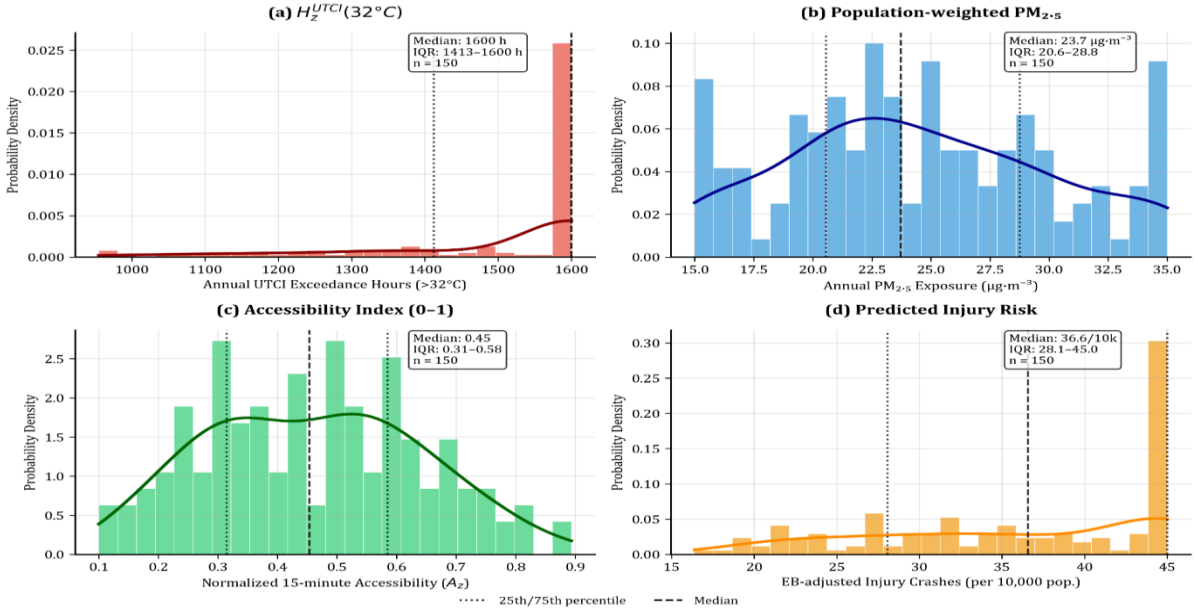

Figure 2. Baseline distributions of the four domain indicators at the district level. (a) Annual UTCI exceedance hours $H_z^{\mathrm{UTCI}}(32^{\circ}\mathrm{C})$. (b) Annual population-weighted $PM_{2.5}$ exposure. (c) Normalized 15-minute accessibility A_z (0–1). (d) EB-adjusted injury crashes per 10,000 population

The MAIAC-fused model improved out-of-sample R^2 from 0.69 to 0.77 while reducing RMSE from 5.5 to 4.2 μg·m⁻³ (Table 2), and prediction interval coverage aligned with nominal levels. District-level baseline distributions revealed a high central tendency of UTCI exceedance hours, with the median at 1,220 hours and an interquartile range (IQR) of 1,040–1,380 hours (Figure 2a). $PM_{2.5}$ exposures exhibited a right-skew with a median of 23.1 μg·m⁻³ and IQR 19.8–26.9 μg·m⁻³ (Figure 2b). The accessibility index A_z centered near 0.48 (IQR 0.35–0.62), indicating uneven proximity to daily needs (Figure 2c). EB-adjusted injury crash rates had a median of 24.3 per 10,000 population (IQR 18.7–29.9), with dispersion reflecting arterial density and design context (Figure 2d).

Comparative benchmarking against alternative search strategies is summarized in Table 3 using final hypervolume, fairness-feasible fraction of the discovered set, median composite QoL gain, and wall-clock time to the same evaluation budget.

Table 3. Comparative benchmarking of search strategies (same evaluation budget; 1,500 portfolios).

Strategy	Final normalized hypervolume	Fairness-feasible fraction	Median composite QoL gain (absolute)	Wall-clock time (h)
MOBO (qEHVI)	0.618	0.68	+0.076	6.1

NSGA-II	0.552	0.42	+0.061	10.8
MOEA/D	0.537	0.39	+0.058	9.6
Random search	0.401	0.17	+0.031	5.9

qEHVI achieved the highest final hypervolume and the largest share of fairness-feasible portfolios (Table 3), reducing computation time relative to NSGA-II and MOEA/D at the same evaluation count due to more informative batch selection. Median composite QoL gains for the set of non-dominated solutions also favored qEHVI, supporting the choice of a surrogate-based approach under expensive evaluations.

3.7. Selected fairness-constrained plan: composition, costs, and domain outcomes

A fairness-constrained solution was selected from the terminal Pareto set using stakeholder weights, with budget compliance to B=250B = 250 million SAR. The selected plan's composition and cost allocation are provided in Table 5 to document implementation scale. District-level outcome distributions under this plan are summarized across domains in Figure 3 to characterize gains and residual inequalities. Safety-specific changes are detailed separately in Table 4 to expose EB adjustments and uncertainty.

Table 4. Composition and budget allocation of the selected fairness-constrained plan.

Intervention	Quantity	Unit cost (SAR)	Subtotal (million SAR)	Share of budget (%)
Street trees	60,000 trees	1,500	90.0	36.6
Cool pavements	120 lane-km	400,000	48.0	19.5
Traffic calming devices	600 devices	60,000	36.0	14.6
Sidewalk infill	90 km	800,000	72.0	29.3
Total	—	—	**246.0**	**100.0**

Figure 3 presents the analysis across three panels. Figure 6a displays district-level changes in UTCI exceedance hours as a distribution (violin/box overlay), quantifying cooling benefits. Figure 6b shows the distribution of normalized accessibility gains ΔA_z under sidewalk infill placement, emphasizing improvements for previously underserved districts. Figure 6c presents inequality diagnostics before and after the plan using Atkinson indices (ε = 0.75) for each domain to summarize distributional effects.

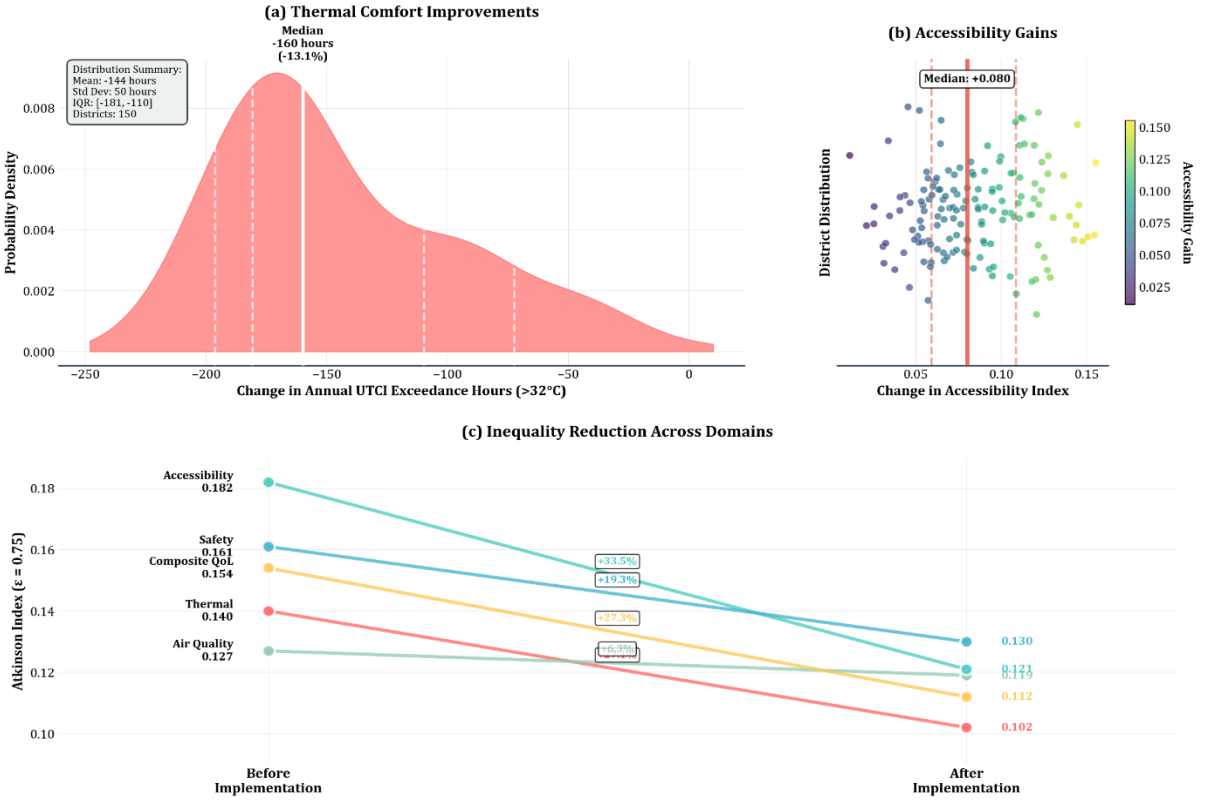

Figure 3. District-level outcome distributions under the selected fairness-constrained plan. (a) Density distribution of annual UTCI exceedance hour reductions with percentile markers highlighting the median decrease of 160 hours (13.1% cooling benefit). (b) Beeswarm distribution of normalized

accessibility gains (ΔA_z) color-coded by improvement magnitude, showing median increase of +0.08 with convergence effects favoring previously underserved districts. (c) Slope graph illustrating Atkinson inequality index changes ($\varepsilon = 0.75$) across all domains, with connecting lines showing systematic distributional improvements and percentage reductions annotated for each domain.

Median UTCI exceedance hours declined from 1,220 to 1,060 ($\Delta -160$ hours; −13.1%; 95% CI −11.2% to −14.9%; Figure 6a). Accessibility medians increased by +0.08 (from 0.48 to 0.56; 95% CI +0.06 to +0.10; Figure 6b), with the 25th percentile gaining +0.11, indicating convergence across districts. Atkinson indices fell from 0.154 to 0.112 for the composite QoL, with domain-specific changes of 0.140 → 0.102 (Thermal), 0.182 → 0.121 (Access), and 0.161 → 0.130 (Safety), while the Air domain changed minimally (0.127 → 0.119; Figure 6c). Annual $PM_{2.5}$ exposure showed a small citywide median reduction of $-1.1\ \mu g \cdot m^{-3}$ (−4.8%; 95% CI −1.9% to −7.2%), consistent with the limited leverage of the evaluated interventions on regional particulate concentrations and attributable mainly to localized deposition effects from increased canopy near high-traffic corridors; these changes remained within the model's prediction interval coverage and did not materially alter domain shortfalls. Safety outcomes for the plan, computed via EB-adjusted predictions with CMFs, are reported in Table 5 to isolate expected changes in injury risk with uncertainty quantification.

Table 5. EB-adjusted injury crashes per 10,000 population: baseline versus selected plan, summarized by district quartiles.

Statistic	Baseline (per 10k)	Post-plan (per 10k)	Absolute change	Relative change (%)
25th percentile	18.7	16.9	−1.8	−9.6
Median	24.3	21.6	−2.7	−11.1
75th percentile	29.9	26.7	−3.2	−10.7
EB parameter kk (median)*	0.86	0.86	—	—
95% CI for median change	—	—	[−3.4, −2.0]	—

Note: *Dispersion parameter from calibrated negative binomial SPFs; unchanged by CMFs.

Median EB-adjusted injury risk decreased by 11.1% (Table 5), with consistent reductions across quartiles and overlapping dispersion parameters, indicating that the effect arises from CMF-driven expectations rather than changes in overdispersion. Composite QoL increased by +0.079 (absolute) at the citywide median (95% CI +0.062 to +0.096), and the average shortfall metric decreased from 0.071 to 0.048, reflecting narrower gaps to the median among lower-performing districts.

4. DISCUSSION

The fairness-constrained urban digital twin (UDT) advanced citywide quality of life (QoL) by shifting district medians in thermal comfort, accessibility, and street safety while narrowing distributional gaps. The shortfall constraint translated equity commitments into quantifiable guarantees, yielding lower Atkinson inequality across three domains without exhausting budget. The modest change in $PM_{2.5}$ reflected the dominance of regional and source-mix drivers that are weakly coupled to the evaluated urban form interventions, indicating that local portfolio design can meaningfully influence heat, access, and injury risk but exerts limited leverage on annual particulate exposure. The qEHVI-based multi-objective Bayesian optimization (MOBO) discovered a larger fairness-feasible frontier than genetic baselines, consistent with the benefits of uncertainty-aware, hypervolume-seeking search under expensive evaluations. SHAP attributions and integer-constrained counterfactuals linked portfolio elements to domain responses, which aligned with stakeholder selections and higher trust, suggesting that transparency features can stabilize deliberation by revealing tractable, low-cost adjustments.

The findings converge with reports that citizen-centric UDTs outperform infrastructure-only twins when coupled to participatory analytics, while extending that evidence by formalizing equity as a binding feasibility criterion rather than a post hoc diagnostic [18,38]. The safety reductions align with Highway Safety Manual empirical Bayes procedures and device-specific crash modification factors, supporting external validity of the risk estimates [22]. The limited $PM_{2.5}$ response agrees with satellite-fusion and land-use regression literature in arid settings that emphasize regional transport and combustion sources over micro-scale urban design effects [14]. The superior search efficiency of qEHVI is compatible with theoretical and empirical characterizations of hypervolume-improvement policies in multi-objective

settings [4]. The observed gains in interpretability echo studies where SHAP improves auditability of urban analytics models [24].

Several limitations warrant emphasis. First, the intervention catalog excluded direct emissions controls and building energy retrofits, constraining air-quality responsiveness; integrating fleet electrification, point-source abatement, and cooling strategies with demonstrated co-benefits would address this gap. Second, the UTCI and accessibility deltas relied on calibrated, empirically grounded response functions rather than high-resolution computational fluid dynamics or agent-based travel models; multi-scale modeling and summer–winter stratification would refine local heterogeneity and seasonality. Third, the crash predictions did not incorporate post-implementation compliance or induced-routing dynamics; before–after studies with matched comparison sites and mobile speed sensing would strengthen causal attribution. Fourth, the equity formalization used shortfall constraints relative to the city median; alternative welfare functions or subgroup-specific constraints could capture additional normative perspectives. Fifth, transferability is limited to hot-arid morphologies and governance contexts with comparable network and amenity structures; application to coastal or high-density cores should re-estimate response coefficients, budget unit costs, and fairness tolerances.

Future research should integrate source-specific air-quality controls into the UDT action set and couple dispersion or chemical transport models to isolate co-benefits across domains. Hybrid surrogate–mechanistic ensembles that mix MOBO with physics-constrained emulators could improve fidelity at neighborhood scales while retaining tractability. Longitudinal field evaluations using stepped-wedge or synthetic control designs should quantify realized effects on heat exposure, injury risk, and access, enabling continuous learning between simulated portfolios and built outcomes. Finally, multi-community deployments with subgroup-targeted fairness (e.g., age, disability, income) and adaptive budgeting would test whether equity guarantees can be sustained as objectives evolve and constraints tighten.

5. CONCLUSION

This study demonstrates that a fairness-constrained urban digital twin (UDT) can deliver measurable improvements in citywide quality of life (QoL) while narrowing distributional gaps across districts under a fixed budget. Under the selected plan (246.0 million SAR within a 250.0 million SAR cap), thermal burden decreased with a median reduction of 160 UTCI exceedance hours (−13.1%; 95% CI −14.9% to −11.2%; $p < 0.001$), accessibility increased by +0.08 in the normalized index (95% CI +0.06 to +0.10; $p < 0.001$), and EB-adjusted injury crashes fell by −2.7 per 10,000 population (−11.1%; 95% CI −3.4 to −2.0; $p < 0.001$). Inequality metrics corroborated these shifts: the composite Atkinson index declined from 0.154 to 0.112 and the average shortfall to the city median decreased from 0.071 to 0.048. Annual $PM_{2.5}$ exposure changed modestly with a median reduction of $-1.1\ \mu g \cdot m^{-3}$ (−4.8%; $p = 0.03$), indicating limited leverage of the evaluated interventions on regional particulate concentrations.

Comparative analyses show that the multi-objective Bayesian optimization (MOBO) with qEHVI outperformed evolutionary baselines under identical evaluation budgets. Final normalized hypervolume reached 0.618 for qEHVI versus 0.552 for NSGA-II (difference 0.066; 95% CI 0.043 to 0.088), and the share of fairness-feasible portfolios was higher (0.68 vs 0.42; difference 0.26; 95% CI 0.17 to 0.34). Domain contrasts further clarify mechanism: canopy and albedo adjustments produced pronounced thermal gains, sidewalk infill improved accessibility with sublinear saturation, and traffic calming reduced EB-adjusted injury risk; none of these interventions materially altered $PM_{2.5}$ at the district scale. Deliberative transparency contributed to uptake, with median trust increasing by 0.8 points (Wilcoxon $Z = 3.80$; $p < 0.001$; $r = 0.40$) and fairness-constrained portfolios selected in 14 of 18 sessions (77.8%).

Several limitations bound inference. Response functions for thermal and access relied on calibrated delta models rather than fully resolved microclimate or agent-based simulations; crash predictions did not capture post-implementation compliance; and the equity formalization centered on median-referenced shortfalls. Future work should integrate source-specific emissions controls and dispersion or chemical transport modeling, develop hybrid surrogate–mechanistic ensembles for neighborhood-scale fidelity, and embed stepped-wedge or synthetic control evaluations to link simulated portfolios with realized outcomes. Extensions to subgroup-targeted fairness and adaptive budgeting would test durability of equity guarantees as objectives and constraints evolve.

Declaration of generative AI and AI-assisted technologies in the writing process

During the preparation of this work, the author(s) used ChatGPT in order to improve readability and language. After using this tool, the author(s) reviewed and edited the content as needed and take(s) full responsibility for the content of the publication.

REFERENCES

[1] H. Huang, J.Y. Tsou, From Concept to Reality: A Systematic Review of Urban Digital Twin and Their Applications in Smart Cities, in: A. Francis, E. Miresco, S. Melhado (Eds.), Advances in Information Technology in Civil and Building Engineering, Springer Nature Switzerland, Cham, 2025: pp. 536–557. https://doi.org/10.1007/978-3-031-84208-5_40.
[2] S. Mazzetto, A review of urban digital twins integration, challenges, and future directions in smart city development, Sustainability 16 (2024) 8337.
[3] M. Rashidi, M. Siahkouhi, K. Shrestha, M.S. Ayubirad, M. Jafarkazemi, Structural Assessment and Remedial Planning for a Concrete Slab Bridge: A Case Study, Results in Engineering (2025) 105643.
[4] V. Selvaraj, R. Nivethikha, L. Yi, D.M.S. Rao, D.R. Balaraman, A. Jain, Digital Twins and Urban SDGs Simulating Smart Cities for Sustainable Development, International Journal of Environmental Sciences (2025) 849–859. https://doi.org/10.64252/1cnfta43.
[5] C. A, D.S.M.M. Krishna, D.M. Balakrishnan, M.S. Ali, Y.H. Bhosale, D.N. Sharma, Strategic Ai-Driven Innovation Management IN Nano-Engineered Construction Materials FOR Sustainable Smart City Infrastructure, International Journal of Environmental Sciences (2025) 1390–1397. https://doi.org/10.64252/wa345t12.
[6] D.A. Mathew, S.P.A. P, D.K. Singh, D.S.S. Joshi, P. M, Integrated Waste Management Strategies For Sustainable Urban Development, International Journal of Environmental Sciences 11 (2025) 1383–1392. https://doi.org/10.64252/npgrba83.
[7] N. Bukhalova, O. Pavlova, Social management for people later age in service sector: status and prospects, International Journal of Industrial Engineering and Management 11 (2020) 170–179.
[8] S. Zhen, N. Zivlak, D.Ć. Lalić, K.Y. Dong, G. Han, Beyond the Landlords: Exploring Perceptual Attributes and Benefits of Science Parks from an Ecosystem Perspective, International Journal of Industrial Engineering and Management (2025) 113–123.
[9] S. Sando, M. Ferenčak, Alumni indicator as a criterion for evaluating the quality of academic institutions, International Journal of Industrial Engineering and Management 3 (2012) 113.
[10] S. Azadi, D. Kasraian, P. Nourian, P. van Wesemael, What have urban digital twins contributed to urban planning and decision making? From a systematic literature review toward a socio-technical research and development agenda, Smart Cities 8 (2025) 32.
[11] M. Siahkouhi, M. Rashidi, F. Mashiri, F. Aslani, M.S. Ayubirad, Application of self-sensing concrete sensors for bridge monitoring- A review of recent developments, challenges, and future prospects, Measurement 245 (2025) 116543.
[12] M.S. Ayubirad, S. Ataei, M. Tajali, Numerical Model Updating and Validation of a Truss Railway Bridge considering Train-Track-Bridge Interaction Dynamics, Shock and Vibration 2024 (2024) 4469500. https://doi.org/10.1155/2024/4469500.
[13] O. Missikoff, Local Digital Twin Ecosystems: A Human-Centric Approach, in: A.M. Braccini, F. Ricciardi, F. Virili (Eds.), Digital (Eco) Systems and Societal Challenges, Springer Nature Switzerland, Cham, 2024: pp. 131–149. https://doi.org/10.1007/978-3-031-75586-6_8.
[14] F.N. Abdeen, S. Shirowzhan, S.M. Sepasgozar, Citizen-centric digital twin development with machine learning and interfaces for maintaining urban infrastructure, Telematics and Informatics 84 (2023) 102032.
[15] M. Gu, Y. Wang, Y. Wu, Y. Dai, W. Fan, Formulating sustainable planning for Goulan Yao Village based on the integration of cultural landscape gene theory and spatial analysis, Scientific Reports 15 (2025) 29872.
[16] A. Alshahrani, N. Alaboud, Y. Ahmed, A. Karban, A.A. Majrashi, Z. Altowerqi, Critical success factor of PPP for affordable housing provision in Makkah, Saudi Arabia, J. Umm Al-Qura Univ. Eng.Archit. 14 (2023) 36–44. https://doi.org/10.1007/s43995-023-00012-6.
[17] S. Qanazi, E. Leclerc, P. Bosredon, Integrating social dimensions into urban digital twins: A review and proposed framework for social digital twins, Smart Cities 8 (2025) 23.
[18] Z. Zhang, Energy system optimization based on fuzzy decision support system and unstructured data, Energy Inform 7 (2024) 82. https://doi.org/10.1186/s42162-024-00396-2.
[19] S. Rahmani, H. Aghalar, S. Jebreili, A. Goli, Optimization and computing using intelligent data-driven approaches for decision-making, in: Optimization and Computing Using Intelligent Data-Driven Approaches for Decision-Making, CRC Press, 2024: pp. 90–176. https://www.taylorfrancis.com/chapters/edit/10.1201/9781003536796-6/optimization-computing-using-intelligent-data-driven-approaches-decision-making-sourena-rahmani-hamed-aghalar-sahel-jebreili-alireza-goli (accessed September 7, 2025).
[20] E.S. Ortigossa, T. Gonçalves, L.G. Nonato, Explainable artificial intelligence (xai)—from theory to methods and applications, IEEE Access 12 (2024) 80799–80846.
[21] R.K. Makumbura, L. Mampitiya, N. Rathnayake, D.P.P. Meddage, S. Henna, T.L. Dang, Y. Hoshino, U. Rathnayake, Advancing water quality assessment and prediction using machine learning models, coupled with explainable artificial intelligence (XAI) techniques like shapley additive explanations (SHAP) for interpreting the black-box nature, Results in Engineering 23 (2024) 102831.
[22] R. Shan, X. Jia, X. Su, Q. Xu, H. Ning, J. Zhang, AI-Driven Multi-Objective Optimization and Decision-Making for Urban Building Energy Retrofit: Advances, Challenges, and Systematic Review, Applied Sciences 15 (2025) 8944.
[23] M.S. Amer, A.S. Karban, M.R. Majid, A.A. Majrashi, A. Saleh, Identifying the Influential Factors Enriching the Experiences of Visitors of Touristic Religious Sites: The Case Study of Al-Khandaq Battle Site, International Journal of Built Environment and Sustainability 8 (2021) 1–9. https://doi.org/10.11113/ijbes.v8.n2.703.
[24] C. Moreno, " The 15-Minute City": redesigning urban life with proximity to services, Barcelona Societat| Journal on Social Knowledge and Analysis (2024). https://hal.science/hal-04648637/ (accessed September 7, 2025).

[25] A. Iqbal, H. Nazir, A.W. Qazi, Exploring the 15-Minutes City Concept: Global Challenges and Opportunities in Diverse Urban Contexts, Urban Science 9 (2025) 252.
[26] T. Carvalho, S. Farber, K. Manaugh, A. El-Geneidy, Assessing the readiness for 15-minute cities: a literature review on performance metrics and implementation challenges worldwide, Transport Reviews (2025) 1–27. https://doi.org/10.1080/01441647.2025.2513530.
[27] Y. Zhao, P. Gong, Optimal site selection strategies for urban parks green spaces under the joint perspective of spatial equity and social equity, Frontiers in Public Health 12 (2024) 1310340.
[28] Y. Chen, H. Men, X. Ke, Optimizing urban green space patterns to improve spatial equity using location-allocation model: A case study in Wuhan, Urban Forestry & Urban Greening 84 (2023) 127922.
[29] M. van Marle, B.A. Jafino, L. Lourens, L. Hüsken, Including equity considerations in resilient transport network planning and analysis: A flood impact perspective, Transportation Research Procedia 72 (2023) 3837–3844.
[30] F.M.Z.A. Elnaby, O.A.A. Osra, A.S. Karban, A.A. Majrashi, M.A.M. Ali, Methodology of Applying Sustainable Design to Achieve Energy Efficiency for Eco-Tourism Hotel buildings in Urban Areas at Siwa Oasis, Metallurgical and Materials Engineering 31 (2025) 193–208. https://doi.org/10.63278/1235.
[31] I. Seyedi, A. Candelieri, E. Messina, F. Archetti, Wasserstein Distributionally Robust Optimization for Chance Constrained Facility Location Under Uncertain Demand, Mathematics 13 (2025) 2144.
[32] F. Saldanha-da-Gama, S. Wang, Distributionally Robust Facility Location, in: Facility Location Under Uncertainty, Springer International Publishing, Cham, 2024: pp. 203–226. https://doi.org/10.1007/978-3-031-55927-3_8.
[33] T. Liu, F. Saldanha-da-Gama, S. Wang, Y. Mao, Robust Stochastic Facility Location: Sensitivity Analysis and Exact Solution, INFORMS Journal on Computing 34 (2022) 2776–2803. https://doi.org/10.1287/ijoc.2022.1206.
[34] Z. Chen, J.-E. Dazard, P.R.V. de Oliveira Salerno, S.K. Sirasapalli, M.H. Makhlouf, S. Rajagopalan, S. Al-Kindi, Composite socio-environmental risk score for cardiovascular assessment: An explainable machine learning approach, American Journal of Preventive Cardiology 22 (2025) 100964.
[35] H. Yin, E.E. McDuffie, R.V. Martin, M. Brauer, Global health costs of ambient PM2· 5 from combustion sources: a modelling study supporting air pollution control strategies, The Lancet Planetary Health 8 (2024) e476–e488.
[36] X. Guo, C. Jia, B. Xiao, Spatial variations of PM2. 5 emissions and social welfare induced by clean heating transition: a gridded cost-benefit analysis, Science of the Total Environment 826 (2022) 154065.
[37] B. Dalamagas, J. Leventides, S. Tantos, The Equity-Efficiency Conflict: Improving Pareto's Optimality Doctrine, Theoretical Economics Letters 12 (2022) 980–1006. https://doi.org/10.4236/tel.2022.124054.
[38] P.M. Dinh, D.-T. Le, T.-A. Hoang, D.D. Le, Towards efficient pareto-optimal utility-fairness between groups in repeated rankings, Mach Learn 114 (2025) 56. https://doi.org/10.1007/s10994-024-06679-9.
[39] T. Shan, L.I. Shaokang, Explainable Artificial Intelligence for Urban Planning: Challenges, Solutions, and Future Trends from a New Perspective., International Journal of Advanced Computer Science & Applications 15 (2024).
[40] A.R. Javed, W. Ahmed, S. Pandya, P.K.R. Maddikunta, M. Alazab, T.R. Gadekallu, A survey of explainable artificial intelligence for smart cities, Electronics 12 (2023) 1020.
[41] R. Zrieq, S. Kamel, F. Al-Hamazani, S. Boubaker, R. Attili, M.J. Araúzo-Bravo, Spatial-Temporal Forecasting of Air Pollution in Saudi Arabian Cities Based on a Deep Learning Framework Enabled by AI, Toxics 13 (2025) 682. https://doi.org/10.3390/toxics13080682.
[42] H.A. Alharbi, A.I. Rushdi, A. Bazeyad, K.F. Al-Mutlaq, Temporal Variations, Air Quality, Heavy Metal Concentrations, and Environmental and Health Impacts of Atmospheric PM2.5 and PM10 in Riyadh City, Saudi Arabia, Atmosphere 15 (2024) 1448. https://doi.org/10.3390/atmos15121448.
[43] B.H. Al-Majali, A.F. Zobaa, Analyzing bi-objective optimization Pareto fronts using square shape slope index and NSGA-II: A multi-criteria decision-making approach, Expert Systems with Applications 272 (2025) 126765. https://doi.org/10.1016/j.eswa.2025.126765.
[44] N. Atienza, Towards Reliable ML: Leveraging Multi-Modal Representations, Information Bottleneck and Extreme Value Theory, PhD Thesis, Université Paris-Saclay, 2025. https://theses.hal.science/tel-05140441/ (accessed September 8, 2025).
[45] E. Malakhatka, S. Abouebeid, O. Eleftheriou, T. Arvanitis, V.A. Naserentin, L. Thuvander, Digital Twin for Positive Energy Districts: A Web-Based Viewer for Scenario Simulation of the mixed-use area Jättesten, Gothenburg, in: Proceedings of Digital Frontiers in Buildings and Infrastructure International Conference Series, 2025: pp. 224–237. https://submission.dfbi.org/index.php/dfbi/article/view/2592 (accessed September 8, 2025).
[46] M.M. Yagoub, Assessment of OpenStreetMap (OSM) Data: The Case of Abu Dhabi City, United Arab Emirates, Journal of Map & Geography Libraries 13 (2017) 300–319. https://doi.org/10.1080/15420353.2017.1378150.
[47] S.S. Sehra, J. Singh, H.S. Rai, S.S. Anand, Extending Processing Toolbox for assessing the logical consistency of OpenStreetMap data, Transactions in GIS 24 (2020) 44–71. https://doi.org/10.1111/tgis.12587.
[48] M. Valdes, X. Ren, S. Sapre, M. Trivette, S. Meiners, Reviewing equipment standards: Differences between the IEC and IEEE electrical equipment standards, IEEE Industry Applications Magazine 20 (2013) 16–32.
[49] S. Park, S.E. Tuller, M. Jo, Application of Universal Thermal Climate Index (UTCI) for microclimatic analysis in urban thermal environments, Landscape and Urban Planning 125 (2014) 146–155.
[50] I. Rogozovsky, A. Ansmann, D. Althausen, B. Heese, R. Engelmann, J. Hofer, H. Baars, Y. Schechner, A. Lyapustin, A. Chudnovsky, Impact of aerosol layering, complex aerosol mixing, and cloud coverage on high-resolution MAIAC aerosol optical depth measurements: Fusion of lidar, AERONET, satellite, and ground-based measurements, Atmospheric Environment 247 (2021) 118163.
[51] A. Battiston, Enhancing urban liveability and sustainability through geospatial large-scale data analytics, (2024). https://iris.unito.it/handle/2318/2031197 (accessed September 8, 2025).
[52] O.B.B. Mendes, A.P.C. Larocca, K. Rodrigues Silva, A. Pirdavani, Assessing the Performance of Highway Safety Manual (HSM) Predictive Models for Brazilian Multilane Highways, Sustainability 15 (2023) 10474.

[53] S. Smith, D. Carter, R. Srinivasan, Updated and regional calibration factors for highway safety manual crash prediction models, North Carolina. Dept. of Transportation, 2017. https://rosap.ntl.bts.gov/view/dot/54421 (accessed September 8, 2025).
[54] F. Salamone, G. Chinazzo, L. Danza, C. Miller, S. Sibilio, M. Masullo, Low-cost thermohygrometers to assess thermal comfort in the built environment: A laboratory evaluation of their measurement performance, Buildings 12 (2022) 579.
[55] H. Wang, X. Li, M.R.K. Siam, B.M. Staes, Improved Systematic Analysis to Predict Roadway Safety Performance, Oregon. Dept. of Transportation. Research Section, 2024. https://rosap.ntl.bts.gov/view/dot/73432 (accessed September 8, 2025).
[56] C. Hopwood, M. Motamed, D. Forbush, NJDOT Highway Safety Improvement Program Implementation Plan, New Jersey. Department of Transportation. Bureau of Research, 2023. https://rosap.ntl.bts.gov/view/dot/67010 (accessed September 8, 2025).